Unconditionally Energy Stable DG-FE Schemes for Diffuse Interface Models

Andreas C. Aristotelous, Ph.D.

Department of Mathematics,
West Chester University, West Chester, PA

Invited Talk

SIAM LS18, Minneapolis, MN.
August 8, 2018

Outline

Sharp Interface

- In classical hydrodynamics, interface is often represented as a discontinuity of density and tangential velocity. (requires jump conditions– interface conditions)

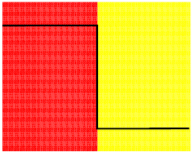

- **sharp** (Young, Laplace):
  - surface of zero thickness
  - discontinuous physical quantities
  - hydrodynamics of bulk fluids coupled with boundary conditions
  - interfacial tension is a jump in stress
  - surface tracking of free boundary

- Leads to singularities when the interfacial thickness becomes comparable to the radius of curvature or the distance between surfaces. (e.g. when material surfaces collide.)
- Real fluids exhibit partial miscibility. They mix on the interface!

Diffuse Interface approach

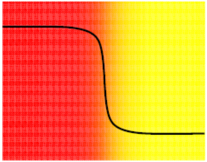

- **diffuse** (Gibbs, van der Waals):
  - surface of non-zero thickness
  - smooth transition of physical quantities
  - hydrodynamics is based on thermodynamic principles
  - interfacial tension is a distributed stress
  - surface capturing

- According to the thermodynamics of "immiscible" fluids, there is a range of concentrations where the free energy is concave and homogeneous states are unstable (e.g. Landau & Lifshitz 1958).
- An interface between two immiscible fluids can then be described as a layer where thermodynamically unstable mixtures are stabilized by weakly non-local (gradient) terms in the energy, an idea which can be traced to van der Waals (1894).
- This approach was first constructively used by Cahn & Hilliard (1958) in the context of a purely diffusional problem. In its original form, the Cahn–Hilliard (CH) equation.

The Cahn-Hilliard Equation (phase separation)

The Cahn-Hilliard equation in mixed formulation (Cahn, Acta Metall., 1961):

$$\begin{aligned} \partial_t u &= \Delta w && \text{in} \quad \Omega, \\ w &= \varepsilon^{-1} u^3 - \varepsilon^{-1} u - \varepsilon \Delta u && \text{in} \quad \Omega, \\ \partial_n u &= \partial_n w = 0 && \text{on} \quad \partial\Omega, \end{aligned}$$

where $\varepsilon > 0$ is the interfacial width parameter.

Mixed weak formulation: find $u \in L^\infty\left(0, T; H^1(\Omega)\right)$, $\partial_t u \in L^2\left(0, T; H^{-1}(\Omega)\right)$ and $w \in L^2\left(0, T; H^1(\Omega)\right)$ such that

$$\begin{aligned} \langle \partial_t u, \chi \rangle + (\nabla w, \nabla \chi) &= 0 && \forall \chi \in H^1(\Omega), \\ \varepsilon^{-1}\left(u^3 - u, \varphi\right) + \varepsilon\left(\nabla u, \nabla \varphi\right) - (w, \varphi) &= 0 && \forall \varphi \in H^1(\Omega), \end{aligned}$$

for almost all $t \in (0, T)$. Note that BCs are natural.

Energy Dissipation and Mass Conservation (PDE level)

Consider the typical Cahn-Hilliard energy (Cahn and Hilliard, J. Chem. Phys., 1957)

$$E(u) = \int_\Omega \left\{ \frac{1}{4\varepsilon} u^4 - \frac{1}{2\varepsilon} u^2 + \frac{1}{4\varepsilon} + \frac{\varepsilon}{2} |\nabla u|^2 \right\} d\mathbf{x}.$$

The chemical potential is

$$w = \delta_u E = \varepsilon^{-1} u^3 - \varepsilon^{-1} u - \varepsilon \Delta u.$$

Weak solutions dissipate the energy at the rate

$$E(u(s)) + \int_0^s \|\nabla w\|_{L^2}^2 \, dt = E(u(0)), \quad \left(d_t E(u) = - \|\nabla w\|_{L^2}^2 \right).$$

Mass conservation:

$$\int_\Omega (u(\mathbf{x},t) - u(\mathbf{x},0)) \, dx = 0, \text{ a.e. } t > 0, \quad \left(d_t \int_\Omega u(\mathbf{x},t) \, d\mathbf{x} = 0 \right).$$

$$E(u) = \int_\Omega \left\{ \frac{1}{4\varepsilon} u^4 - \frac{1}{2\varepsilon} u^2 + \frac{1}{4\varepsilon} + \frac{\varepsilon}{2} |\nabla u|^2 \right\} d\mathbf{x}.$$

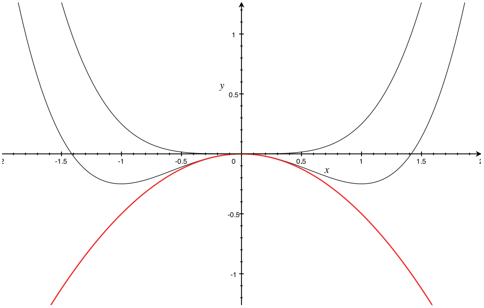

Spinodal Decomposition

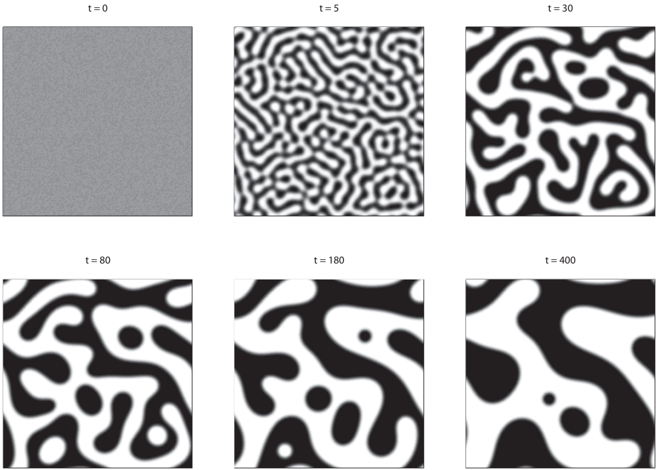

Modified Cahn-Hilliard Equation Models

A Modified Cahn-Hilliard (MCH) Equation

A model for binary polymer dynamics (Ohta & Kawasaki, Macromolecules, 1986; Choksi *et al.*, SIADS, 2011):

$$
\begin{aligned}
\partial_t u &= \Delta w - \theta\left(u - \overline{u}_0\right) && \text{in} \quad \Omega, \\
w &= \varepsilon^{-1} u^3 - \varepsilon^{-1} u - \varepsilon \Delta u && \text{in} \quad \Omega, \\
\partial_n u &= \partial_n w = 0 && \text{on} \quad \partial\Omega,
\end{aligned}
$$

where $\varepsilon > 0$, $\theta \geq 0$, $\overline{u}_0 := \frac{1}{|\Omega|} \int_\Omega u(\mathbf{x}, 0) d\mathbf{x}$.

Mixed weak formulation: find $u \in L^\infty\left(0, T; H^1(\Omega)\right)$, $\partial_t u \in L^2\left(0, T; H^{-1}(\Omega)\right)$ and $w \in L^2\left(0, T; H^1(\Omega)\right)$ such that

$$
\begin{aligned}
\langle \partial_t u, \chi \rangle + (\nabla w, \nabla \chi) + \theta\left(u - \overline{u}_0, \chi\right) &= 0 && \forall \chi \in H^1(\Omega), \\
\varepsilon^{-1}\left(u^3 - u, \varphi\right) + \varepsilon\left(\nabla u, \nabla \varphi\right) - (w, \varphi) &= 0 && \forall \varphi \in H^1(\Omega),
\end{aligned}
$$

for almost all $t \in (0, T)$.

Energy Dissipation and Mass Conservation

Solutions of the MCH equation dissipate the energy

$$E(u) = \int_\Omega \left\{ \frac{1}{4\varepsilon} u^4 - \frac{1}{2\varepsilon} u^2 + \frac{\varepsilon}{2} |\nabla u|^2 \right\} d\mathbf{x} + \frac{\theta}{2} \|u - \overline{u}_0\|_{H^{-1}}^2$$

at the rate

$$E\big(u(s)\big) + \int_0^s \|\partial_t u\|_{H^{-1}}^2 \, dt = E\big(u(0)\big), \quad \left(d_t E(u) = -\|\partial_t u\|_{H^{-1}}^2\right).$$

Mass conservation: For a.e. $t > 0$,

$$0 = \int_\Omega (u(\mathbf{x}, t) - u(\mathbf{x}, 0))\, dx = \int_\Omega (u(\mathbf{x}, t) - \overline{u}_0)\, dx.$$

Spinodal Decomposition and Arrested Coarsening

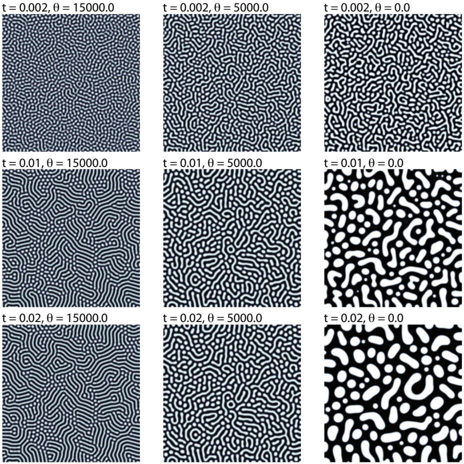

Here $\overline{u}_0 = -0.1$, $\Omega = (0,8)^2$, $\varepsilon = 0.02$, $h = \frac{8}{512}$, $\tau = 2 \times 10^{-5}$.

$\overline{u}_0 = -0.3$, $\theta = 15000.0$, $\Omega = (0,8)^2$, $\varepsilon = 0.02$, $h = \frac{8}{512}$, $\tau = 2 \times 10^{-5}$.

$\overline{u}_0 = -0.3$, $\theta = 15000.0$, $\Omega = (0,8)^2$, $\varepsilon = 0.02$, $h = \frac{8}{512}$, $\tau = 2 \times 10^{-5}$.

$\overline{u}_0 = -0.3$, $\theta = 15000.0$, $\Omega = (0, 8)^2$, $\varepsilon = 0.02$, $h = \frac{8}{512}$, $\tau = 2 \times 10^{-5}$.

$\overline{u}_0 = -0.3$, $\theta = 15000.0$, $\Omega = (0,8)^2$, $\varepsilon = 0.02$, $h = \frac{8}{512}$, $\tau = 2 \times 10^{-5}$.

$\overline{u}_0 = -0.3$, $\theta = 15000.0$, $\Omega = (0, 8)^2$, $\varepsilon = 0.02$, $h = \frac{8}{512}$, $\tau = 2 \times 10^{-5}$.

$\overline{u}_0 = -0.3$, $\theta = 15000.0$, $\Omega = (0,8)^2$, $\varepsilon = 0.02$, $h = \frac{8}{512}$, $\tau = 2 \times 10^{-5}$.

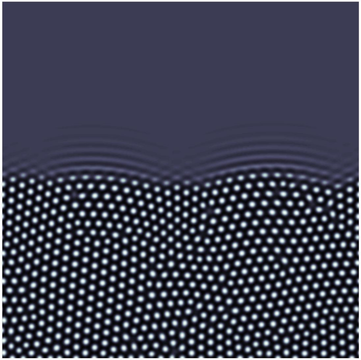

$\overline{u}_0 = -0.3,\ \theta = 15000.0,\ \Omega = (0,8)^2,\ \varepsilon = 0.02,\ h = \frac{8}{512},\ \tau = 2 \times 10^{-5}.$

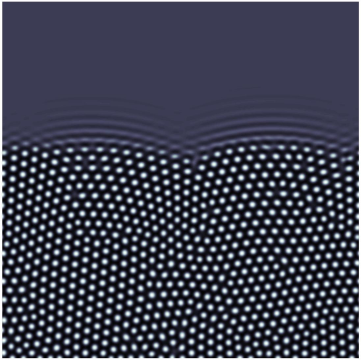

$\overline{u}_0 = -0.3$, $\theta = 15000.0$, $\Omega = (0,8)^2$, $\varepsilon = 0.02$, $h = \frac{8}{512}$, $\tau = 2 \times 10^{-5}$.

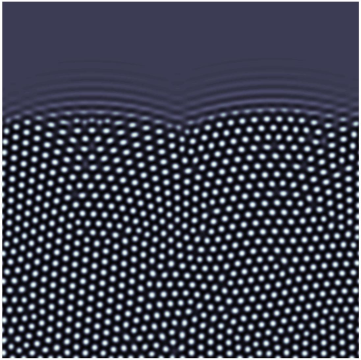

$\overline{u}_0 = -0.3$, $\theta = 15000.0$, $\Omega = (0, 8)^2$, $\varepsilon = 0.02$, $h = \frac{8}{512}$, $\tau = 2 \times 10^{-5}$.

Mathematical Ingredients

- Mass transport (conservation of mass)

$$\text{change in mass} = (\text{transport (in) of mass}) + (''\text{creation}'' \text{ of mass})$$

$$\frac{\partial c_i}{\partial t} + \nabla \cdot (\mathbf{u} c_i) = \nabla \cdot (D_i \nabla c_i) - r_i, \quad (\text{solvent}),$$

$$\frac{\partial}{\partial t} X_j + \nabla \cdot (\mathbf{u}_j X_j) = \nabla \cdot (\kappa_j \nabla X_j) + g_j, \quad (\text{biomaterial}).$$

- Force balance (conservation of momentum)

$$\begin{aligned} 0 \quad = \quad & (\text{inertial force}) + (\text{transport of momentum}) + (\text{viscous force}) \\ & + (\text{elastic force}) + (\text{cohesive force}) + \ldots \end{aligned}$$

needed to determine velocities $\mathbf{u}$, $\mathbf{u}_j$.

all in a moving bdry/interface problem (can be complicated!).

Model with nutrient diffusion & advective velocity

$$\begin{aligned}
\partial_t u &= \triangle\mu + S - \nabla\cdot(u\vec{U}), \quad \text{in } \Omega_T := \Omega\times(0,T) \\
\text{where, } S &= \eta\lambda_e u - \lambda_c u, \ \lambda_e > 0, \ \lambda_c > 0 \\
\mu &= f(u) - \epsilon^2\triangle u \\
\triangle\eta &= \lambda_\eta u\eta \quad \text{with} \quad \eta = 1 \quad \text{on} \quad \partial\Omega \\
\vec{U} + \nabla\Pi &= -\lambda u\nabla\mu, \ \Pi\text{: pressure} = 0 \text{ on } \partial\Omega \text{ Darcy equation} \\
\nabla\cdot\vec{U} &= S \quad \text{Mass conservation} \\
u &= u_0, \quad \text{on } \Omega\times\{0\} \\
\partial_n u = \partial_n\mu &= 0, \quad \text{on } \partial\Omega_T := \partial\Omega\times(0,T) \\
f &= F', \ \text{where } F(u) = \frac{1}{4}u^2(1-u)^2.
\end{aligned}$$

Heterogeneous Living Materials

- Phase separation of binary fluid in "Brinkman" porous medium. (CH-B):

$$
\begin{aligned}
\partial_t \psi &= \nabla \cdot (\varepsilon M(\psi) \nabla w - \mathbf{u}\psi), \\
-\nabla \cdot [\nu(\psi) \mathrm{D}(\mathbf{u})] + \eta(\psi)\mathbf{u} &= -\nabla p - \lambda \psi \nabla w, \\
\nabla \cdot \mathbf{u} &= 0.
\end{aligned}
$$

- $\psi = X_j$ for some j, M: mobility, $\mathbf{u}$: fluid velocity, $\mathrm{D}(\mathbf{u}) = \nabla \mathbf{u} + \nabla \mathbf{u}^T$, p: fluid pressure, $\lambda \geq 0$: excess surface tension, $\nu(\,\cdot\,) \geq 0$: fluid viscosity and $\eta(\,\cdot\,) \geq 0$: permeability.
- $\eta \equiv 0$, equation is called the Cahn-Hilliard-Stokes (CH-S) equation.
- $\nu \equiv 0$, obtain Cahn-Hilliard-Hele-Shaw (CH-HS) equation.
- Model growth: $\nabla \cdot \mathbf{u} = S$ and $\partial_t \psi = \nabla \cdot (\varepsilon M(\psi) \nabla w - \mathbf{u}\psi) + S$.

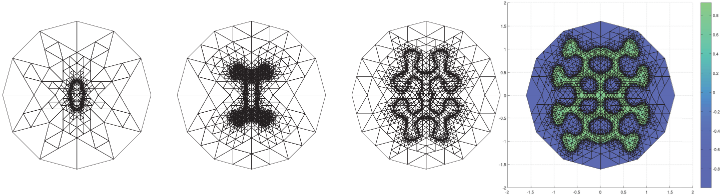

Figure: A 6-level mesh adaptive Discontinuous Galerkin Finite Element simulation of growth. Aristotelous et al., IMA J. Numer. Anal. (2015)

Numerical Solution of the Models

Challenges:

- Nonlinearities
- Fourth Order Operators Generate Ill-conditioned Systems
- Steep Gradients Along the Interfaces, ($\epsilon << diam(\Omega)$)
- Long Time Dynamics Require High Order Stable Schemes
- 3D Formulation and Implementation

Why DGFE Methods for Spatial Discretization?

1. Result in dimension independent formulations.
2. Can easily handle boundary conditions and curved boundaries.
3. It creates matrices that have well structured blocks, so they are easier to handle.

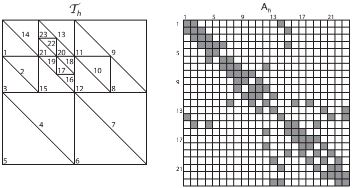

Figure: *Block structure of the stiffness matrix.*

4. Inter-mesh operations, (e.g. projections from a locally refined mesh to a coarse mesh), are entirely local, important in the multigrid setting.
5. Highly parallelizable algorithms

DGFE Triangulations

DG allows the use of more flexible meshes that have hanging nodes.
Let $\mathcal{T}_h = \{K\}$ be a (not necessarily conforming) family of triangulations of Ω, where $0 < h < 1$, $h = \max_{K \in \mathcal{T}_h} h_K$, $h_K = \mathrm{diam}\,(K)$.

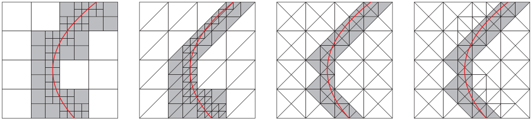

Assume that $\mathcal{T}_h$ satisfies:

1. The elements (cells) of $\mathcal{T}_h$ satisfy the minimal angle condition
2. $\mathcal{T}_h$ is locally quasi-uniform. That is, if two cells K and K' are adjacent, then $h_K \approx h_{K'}$.

Define

$$\mathcal{E}^I := \text{ set of all interior edges/faces of } \mathcal{T}_h.$$

DGFE Function Spaces

Broken Sobolev spaces:

$$H^m(\mathcal{T}_h) := \prod_{K \in \mathcal{T}_h} H^m(K) = \left\{ v \in L^2(\Omega) \;\middle|\; v|_K \in H^m(K) \right\}.$$

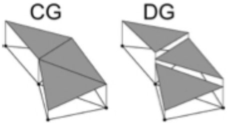

(Pic by Dr. Thomas Lewis, UNCG)

Broken polynomial spaces:

$$V_h := S(\mathcal{T}_h) := \mathcal{P}_q(\mathcal{T}_h) := \prod_{K \in \mathcal{T}_h} P_q(K) = \left\{ v \in L^2(\Omega) \;\middle|\; v|_K \in P_q(K) \right\}.$$

E.g. for $m = 2$, clearly

$$S(\mathcal{T}_h) \subset H^2(\mathcal{T}_h) \subset L^2(\Omega),$$
$$S(\mathcal{T}_h) \not\subset H^2(\Omega), \quad S(\mathcal{T}_h) \not\subset H^1(\Omega).$$

SIPDG Bilinear Form and Broken Norm

For all $u,\ v \in H^2\left(\mathcal{T}_h\right)$, define the symmetric semi positive definite bilinear form

$$\begin{aligned}\alpha_h(u,v) \quad := \quad & \sum_{K\in\mathcal{T}_h}(\nabla u,\nabla v)_K - \sum_{e\in\mathcal{E}^I}\Big(\langle\{\partial_n u\},[v]\rangle_e + \langle[u],\{\partial_n v\}\rangle_e\Big) \\ & + \sum_{e\in\mathcal{E}^I}\gamma h_e^{-1}\langle[u],[v]\rangle_e,\end{aligned}$$

where γ is a positive penalty parameter.

Consistency: If $u \in H^2(\Omega)$, $\partial_n u = 0$ on $\partial\Omega$,

$$-\left(\Delta u, v\right) = \alpha_h(u,v)\,, \quad \forall\ v \in H^2\left(\mathcal{T}_h\right).$$

For all $v \in H^2\left(\mathcal{T}_h\right)$ define

$$|||v|||^2 := \sum_{K\in\mathcal{T}_h}\left(\nabla v,\nabla v\right)_K + \sum_{e\in\mathcal{E}^I}\left(2\frac{\gamma}{h_e}|[v]|_e^2 + \frac{h_e}{\gamma}|\{\nabla v\}|_e^2\right).$$

Mixed SIP-DGFE Convex Splitting Scheme for the MCH

Aristotelous, A. C., O. Karakashian, and S.M. Wise, *A Mixed Discontinuous Galerkin, Convex Splitting Scheme for a Modified Cahn-Hilliard Equation and an Efficient Nonlinear Multigrid Solver*, DCDS-B (Vol. 18, No. 9) November 2013, pp. 2211–2238.

Fully discrete convex splitting scheme

For any $1 \leq m \leq M$, given $u_h^{m-1} \in S(\mathcal{T}_h)$ find $u_h^m, w_h^m \in S(\mathcal{T}_h)$ such that

$$\begin{aligned} (\delta_\tau u_h^m, \chi) + \alpha_h(w_h^m, \chi) + \theta\,(u_h^m - \overline{u}_0, \chi) &= 0, && \forall \chi \in S(\mathcal{T}_h), \\ \varepsilon^{-1}\left((u_h^m)^3 - u_h^{m-1}, \varphi\right) + \varepsilon\alpha_h(u_h^m, \varphi) - (w_h^m, \varphi) &= 0, && \forall \varphi \in S(\mathcal{T}_h), \end{aligned}$$

where

$$u_h^0 := P_h u_0.$$

$P_h : H^2(\mathcal{T}_h) \to S(\mathcal{T}_h)$ is the elliptic projection:

$$\alpha_h(P_h u - u, \chi) = 0, \quad \forall \chi \in S(\mathcal{T}_h), \quad (P_h u - u, 1) = 0.$$

It is easy to see that the scheme is discretely mass conservative:

$$(u_h^m - \overline{u}_0, 1) = 0, \quad \forall\ m \geq 1.$$

Results of the Analysis of the Scheme

Unconditional Unique Solvability

Theorem (Aristotelous et al., 2013)

The mixed SIP-DGFE-CS scheme is uniquely solvable for any mesh parameters τ *and* h *and for any phase parameters* $\theta \geq 0$ *and* $\varepsilon > 0$*.*

Proof.

Set $u_h^m = v_h^m + \overline{u}_0$, $v_h^m \in \mathring{S}(\mathcal{T}_h)$, $m = 0, \ldots, M$. For all $v_h \in \mathring{S}(\mathcal{T}_h)$, define the functional

$$G_h(v_h) := \frac{\tau}{2\beta}\left\|\frac{\beta v_h - v_h^{m-1}}{\tau}\right\|_{-1,h}^2 + \frac{1}{4\varepsilon}\left\|v_h + \overline{u}_0\right\|_{L^4}^4 + \frac{\varepsilon}{2}|||v_h|||_\alpha^2 - \frac{1}{\varepsilon}\left(v_h^{m-1} + \overline{u}_0, v_h\right), \quad \beta := 1 + \tau\theta.$$

G_h is strictly convex and coercive on the linear subspace $\mathring{S}(\mathcal{T}_h)$. Consequently, G_h has a unique minimizer, call it $v_h^m \in \mathring{S}(\mathcal{T}_h)$. □

Unconditional Energy Stability

Lemma (**Aristotelous et al.**, 2013)

Let $u_h^m, w_h^m \in S(\mathcal{T}_h)$ *denote the unique solution of the mixed SIP-DGFE-CS scheme. Then the following energy law holds for any* τ, $h > 0$ *and any* $\theta \geq 0$ *and* $\varepsilon > 0$*:*

$$\begin{aligned} E_h\left(u_h^\ell\right) + \tau \sum_{m=1}^{\ell} \|\delta_\tau u_h^m\|_{-1,h}^2 + \tau^2 \sum_{m=1}^{\ell} \Bigg\{ & \frac{\varepsilon}{2} |||\delta_\tau u_h^m|||_\alpha^2 + \frac{1}{4\varepsilon} \left\|\delta_\tau (u_h^m)^2\right\|_{L^2}^2 \\ & + \frac{1}{2\varepsilon} \|u_h^m \delta_\tau u_h^m\|_{L^2}^2 + \frac{1}{2\varepsilon} \|\delta_\tau u_h^m\|_{L^2}^2 + \frac{\theta}{2} \|\delta_\tau u_h^m\|_{-1,h}^2 \Bigg\} \\ & = E_h\left(u_h^0\right), \quad \forall\ 0 \leq \ell \leq M, \end{aligned}$$

where

$$E_h(u_h) := \frac{1}{4\varepsilon} \left\|(u_h)^2 - 1\right\|_{L^2}^2 + \frac{\varepsilon}{2} |||u_h|||_\alpha^2 + \frac{\theta}{2} \|u_h - \overline{u}_0\|_{-1,h}^2 .$$

Discrete Energy Dissipation (Crystallization)

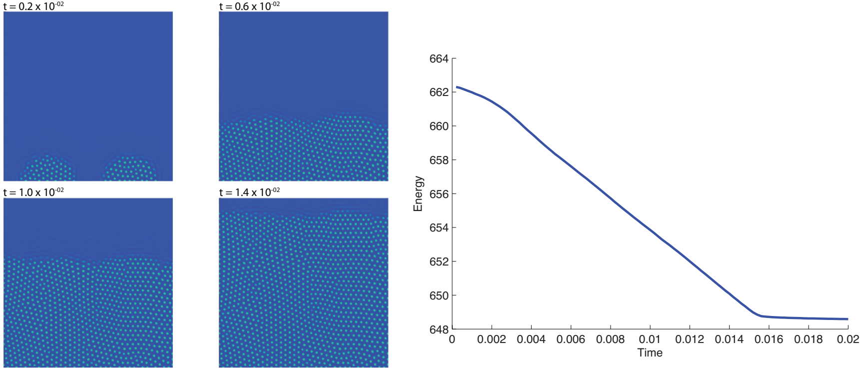

(a) (b)

Unconditional Uniform Bounds on the DG Solution

Lemma (Aristotelous et al., 2013)

Let $u_h^m, w_h^m \in S(\mathcal{T}_h)$ be the unique solution of the mixed SIP-DGFE-CS scheme. Then the following estimates hold for any $h, \tau > 0$:

$$\max_{0\le m\le M}\left[\varepsilon |||u_h^m|||_\alpha^2 + \frac{1}{4\varepsilon}\left\|(u_h^m)^2 - 1\right\|_{L^2}^2 + \frac{\theta}{2}\|u_h^m - \overline{u}_0\|_{-1,h}^2\right] \le C,$$

$$\max_{0\le m\le M}\left(\|u_h^m\|_{L^2}^2 + |||u_h^m|||_\alpha^2\right) \le C,$$

$$\tau\sum_{m=1}^{M}\|\delta_\tau u_h^m\|_{-1,h}^2 \le C,$$

for some h, τ, and T-independent constant $C > 0$.

Convergence

Theorem (Aristotelous et al., 2013)

Let $p \geq 1$ and $1 \leq s \leq p$. Suppose $u_0 \in H^{s+1}(\Omega)$ and (u, w) is a weak solution to the Modified CH equation, with sufficient additional regularities. Then, provided $0 < \tau < \tau_0$, for some τ_0 sufficiently small,

$$\|u - u_{h,\tau}\|_{L^\infty(0,T;H^1(\mathcal{T}_h))} + \|w - w_{h,\tau}\|_{L^2(0,T;H^1(\mathcal{T}_h))} \leq C(T)(h^s + \tau),$$

for all $1 \leq s \leq p$, for some $C(T) > 0$ that is independent of τ and h.

Numerical Convergence Tests

Broken H^1 Convergence Test: Quadratic Elements

Broken H^1 Convergence Test: $q = 2$				
Analytic solution: $u(x,y,t) = x^2(1-x)^2y^2(1-y)^2\cos(t)$				
	$\tau = h^2$		$\tau = h$	
h	$\lvert\lvert\lvert u(\cdot,T) - u_h^M \rvert\rvert\rvert$	rate	$\lvert\lvert\lvert u(\cdot,T) - u_h^M \rvert\rvert\rvert$	rate
1/2	3.122755×10^{-04}	—	5.201555×10^{-04}	—
1/4	7.389662×10^{-05}	2.079239103	2.426696×10^{-04}	1.099949591
1/8	1.835997×10^{-05}	2.008944676	1.195414×10^{-04}	1.021483045
1/16	4.581559×10^{-06}	2.002653198	5.945521×10^{-05}	1.007635202
1/32	1.144499×10^{-06}	2.001122396	2.966275×10^{-05}	1.003150883

Table: $T = 1.5$, $\varepsilon = 0.5$, $\theta = 0$, $\Omega = (0,1)^2$. The global error at T measured in $\lvert\lvert\lvert \cdot \rvert\rvert\rvert$ is expected to be $O(\tau = h^2) + O(h^2)$ (quadratic convergence) and $O(\tau = h) + O(h^2)$ (linear convergence), respectively. The data above are consistent with these predictions.

Second Order in Time CS for the CH

Based on Crank Nicolson formulation

(see e.g. A. Diegel, et al., IMJNA, 2016 for standard FE),

$$\psi^{k+1} - \psi^k = \tau \Delta w^{k+\frac{1}{2}} \ ,$$

$$w^{k+\frac{1}{2}} = \frac{1}{2}\left[\left(\psi^{k+1}\right)^2 + \left(\psi^k\right)^2\right] \psi^{k+\frac{1}{2}} - \tilde{\psi}^{k+\frac{1}{2}} - \varepsilon^2 \Delta \hat{\psi}^{k+\frac{1}{2}} \ ,$$

where

$\psi^{k+\frac{1}{2}} := \frac{1}{2}\psi^{k+1} + \frac{1}{2}\psi^k$, $\tilde{\psi}^{k+\frac{1}{2}} := 3/2\psi^k - \frac{1}{2}\psi^{k-1}$ and $\hat{\psi}^{k+\frac{1}{2}} := 3/4\psi^k + 1/4\psi^{k-1}$.

Based on BDF formulation

(see Yan et al., Commun. Comput. Phys., 2018 for standard FE),

$$3\psi^{k+1} - 4\psi^k + \psi^{k-1} = 2\tau \Delta w^{k+1} \ ,$$

$$w^{k+1} = \left(\psi^{k+1}\right)^3 - 2\psi^k + \psi^{k-1} - \varepsilon^2 \Delta \psi^{k+1} - \tau A \Delta(\psi^{k+1} - \psi^k) \ ,$$

where $A \geq 1/16$ for stability.

BDFCS2-SIP-DG-FE Convergence Test: Linear Elements

2D Analytic solution: $u(x, y, t) = \cos(\pi x) \cos(\pi y) \exp(-t)$ in $(0, 1)^2$ using $\varepsilon^2 = 0.05$ and a linear path $\tau = 0.25h$. Error is of order $O(h^2 + \tau^2) = O(h^2)$

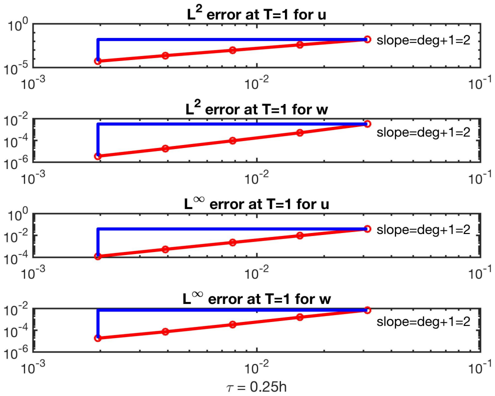

Note: SIP-DG-FE theoretical numerical analysis of both schemes is in progress.

3D Spinodal Snapshot using the BDFCS2-SIP-DG-FE

In $(0,1)^3$ using $\varepsilon^2 = 0.0004$, linear elements and uniform grid $30 \times 30 \times 30$.

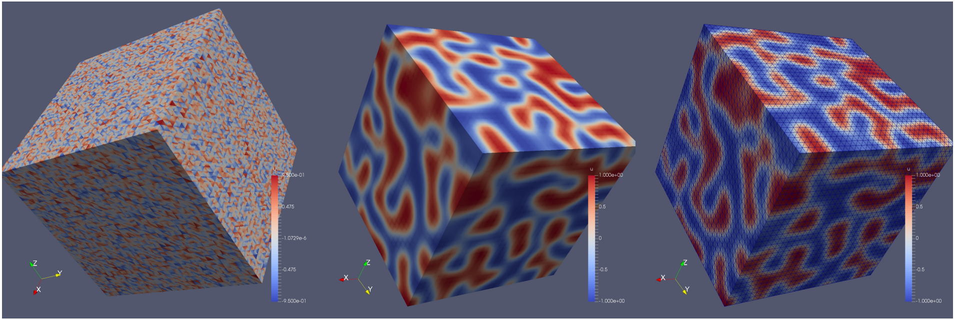

Note: Observe that the mesh size needs to be finer for better resolution of the interface. In 3D uniform mesh is very costly! Needs mesh adaptivity.

Spatially Adaptive Discontinuous Galerkin Methods for a Growth Model

Aristotelous, A. C., O. Karakashian, and S.M. Wise, *Adaptive, Second-Order in Time, Primitive-Variable Discontinuous Galerkin Schemes for a Cahn-Hilliard Equation with a Mass Source*
(IMA J. Num. Anal.) 2015

See also Feng and Karakashian, Math of Comp, 2007.

Simplified Growth Model

Cahn-Hilliard Equation with Nonlinear Mass Source (Cohen & Murray, J. Math. Biol., 1981; Ochoa & Robles, Kinam Rev. Fís., 1983; Wise et. al., J. Theor. Biol., 2008; ACA, IMAJNA 2015)

$$
\begin{aligned}
\partial_t u &= D\Delta w + \frac{1}{\varepsilon}\sigma(u), \\
w &= \varepsilon^{-1}u^3 - \varepsilon^{-1}u - \varepsilon\Delta u, \\
\text{where, } \sigma(u) &:= \lambda_g (u-1)^2(u+1)^2 - \lambda_d \frac{u+1}{2}.
\end{aligned}
\tag{1}
$$

- This is a phenomenological model of biological growth, in particular **solid tumor growth**.
- Models **cell-cell adhesion**, growth and necrosis, without considering mechanical response due to tissue growth.
- Similar to the MCH equation, at the PDE level, this model has an energy which its solutions dissipate.

Reason for Adaptivity

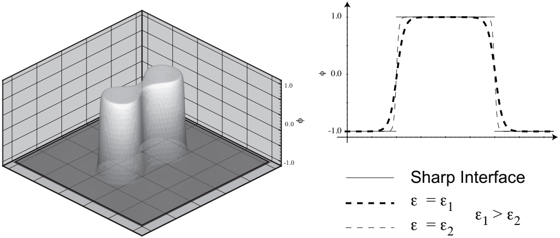

Adaptive Implementation

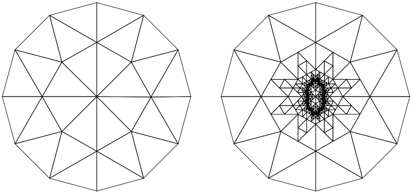

Figure: *Left: Initial mesh used to generate the adaptive multilevel meshes for the simulations. The domain is a dodecagon with "radius" equal to* 1.6*. Right: Resolved ellipse initial profile.*

Time Stepping and Adaptivity Setup

- Let $I_m := (t^{m-1}, t^m]$, $m = 1, \dots, M$ be a partition of $[0, T]$ and $\tau_m := t^m - t^{m-1}$.
- At certain times t^m, the spatial mesh may be changed $\mathcal{T}_h^{m-1} \to \mathcal{T}_h^m$ via a process of refinement and coarsening based on a marking strategy.

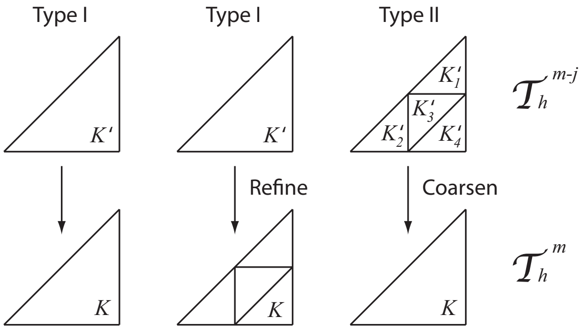

Figure: Examples of type I and type II cells in a two-dimensional mesh.

Error Estimates (Accounting Mesh Adaptivity)

Theorem (Aristotelous et al. 2015)

Let u solves the tumor model with sufficient regularity assumptions and let the fully discrete approximations $\{U^m\}_{m=1}^M$ with f, σ replaced by f_L, σ_L and U^0, U^1 (chosen appropriately). Then for τ and h sufficiently small the following estimate holds for the error $e^m := u(t^m) - U^m$

$$\max_{1\le m\le M} \|e^m\| \le c\, \mathrm{e}^{C_\varepsilon T} \left(\tau^2 + h^r + \mathcal{N}_c \max_{2\le m\le M} \|[w_h^{m-1}]\|\right), \tag{2}$$

where the constant C_ε is proportional to $\frac{1}{\varepsilon^3}$ and $\mathcal{N}_c$ denotes the total number of times where the jumps $[w_h^{m-1}]$ are nonzero.

There exists a constant c_0 such that if also

$$h_{min}^{-\frac{d}{2}} \left(\tau^2 + h^r + \mathcal{N}_c \max_{2\le m\le M} \|[w_h^{m-1}]\|\right) \le c_0,$$

then the estimate (2) also holds for the unmodified schemes.

Inverse Estimate Marking Strategy

Lemma

There exists a constant c depending only on the minimum angle of K and r such that

$$\|u_h\|_{j,K} \le c h_K^{-j} \|u_h\|_K \quad \forall u_h \in P_{r-1}(K),\ j = 1, \dots, r-1.$$

We have the following,

$$c_K := h_K \frac{||\nabla u_h||_K}{||u_h + const||_K} \le C.$$

Adding a constant function on u_h to avoid division by zero.

- if $c_K \le \Theta_c C$ then coarsen.
- if $c_K \ge \Theta_R C$ then refine.

See J. L. Bona, V. A. Dougalis, O. A. Karakashian, and W. R. McKinney,1990.

Adaptive DG Computations of Growth

(Loading tumor.avi)

Parameters: $\varepsilon = 0.0125$, $D = 0.25$, $\lambda_g = 70$ and $\lambda_d = 23$.

Computational Gain

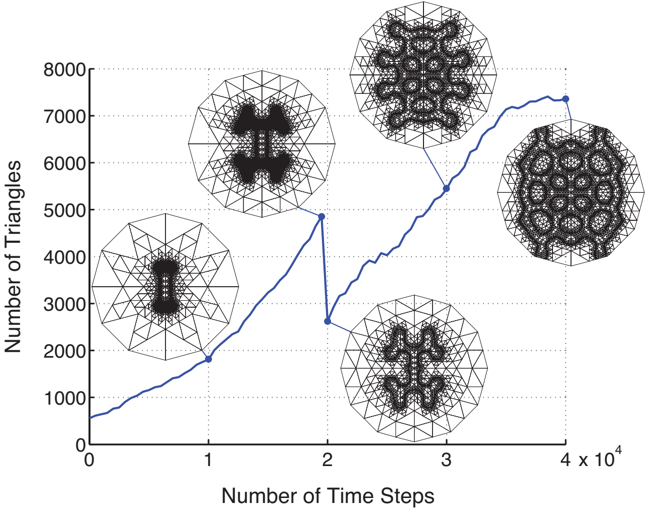

Figure: Adaptive run for growth model.

Solution Sinking

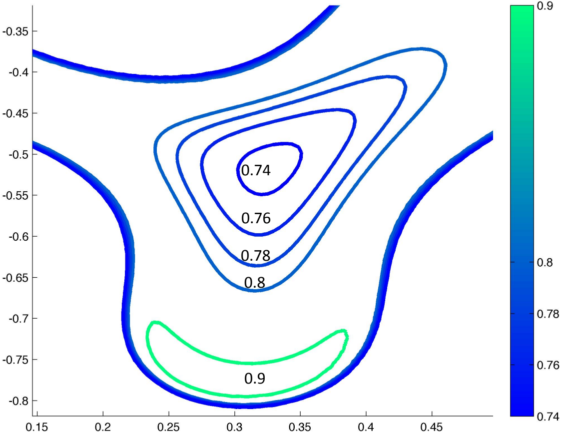

Figure: Contour lines for the solution at $t = 19500\tau$ for the simulation depicted in the last two figures. Shown are the 5 contours 0.74, 0.76, 0.78, 0.8 and 0.9.

An Adaptive Full Approximation Storage (AFAS) Multigrid Solver

AFAS/FD mixed CH: S.M. Wise, J.S. Kim, and J.S. Lowengrub, JCP, 2007.

Uniform Mesh FAS/FD mixed CH: J.S. Kim, K. Kang, and J.S. Lowengrub, JCP, 2004.

The nonlinear algebraic system resulting from the convex splitting scheme, after dropping the superscripts, is

$$\begin{aligned} (1+\tau\theta)\mathrm{M}_h\mathbf{u}_h + \tau\mathrm{A}_h\mathbf{w}_h &= \mathbf{s}_h^u, \\ \varepsilon\mathrm{A}_h\mathbf{u}_h + \varepsilon^{-1}\mathrm{Q}_h(\mathbf{u}_h)\,\mathbf{u}_h - \mathrm{M}_h\mathbf{w}_h &= \mathbf{s}_h^w, \end{aligned}$$

where the source terms, $\mathbf{s}_h^\phi$ and $\mathbf{s}_h^\mu$, involve the previous-time solution $\mathbf{u}_h^k$.

- A_h is the (fine-level) symmetric stiffness matrix: the (i,j) entry is $\alpha_h(u_{h,j}, u_{h,i})$.
- $\mathrm{Q}_h(\mathbf{v}_h)$ is the symmetric positive semidefinite matrix whose (i,j) entry is $\left(v_h^2\ u_{h,j}, u_{h,i}\right)$.
- $\mathrm{M}_h := \mathrm{Q}_h(\mathbf{1})$ is the mass matrix.

(Non-linear) Block Smoothing Strategy

The vectors $\mathbf{u}_t^\ell$, $\mathbf{w}_t^\ell$ are updated element (triangle)-wise by the following block Gauss-Seidel smoothing strategy: for every $t = 1, \ldots, n_h$, for $\ell = 1, \ldots, \ell_{\max}$, find $\mathbf{u}_t^\ell$ and $\mathbf{w}_t^\ell$, such that

$$
\begin{aligned}
(1+\tau\theta)\mathsf{M}_{t,t}\mathbf{u}_t^\ell + \tau \mathsf{A}_{t,t}\mathbf{w}_t^\ell =& \mathbf{s}_t^u - \tau \sum_{t'=1}^{t-1} \mathsf{A}_{t,t'}\mathbf{w}_{t'}^\ell \\
& - \tau \sum_{t'=t+1}^{n_h} \mathsf{A}_{t,t'}\mathbf{w}_{t'}^{\ell-1}, \\
\left[\epsilon \mathsf{A}_{t,t} + \epsilon^{-1}\mathsf{Q}_{t,t}\left(\mathbf{u}_t^{\ell-1}\right)\right]\mathbf{u}_t^\ell - \mathsf{M}_{t,t}\mathbf{w}_t^\ell =& \mathbf{s}_t^w - \epsilon \sum_{t'=1}^{t-1} \mathsf{A}_{t,t'}\mathbf{u}_{t'}^\ell \\
& - \epsilon \sum_{t'=t+1}^{n_h} \mathsf{A}_{t,t'}\mathbf{u}_{t'}^{\ell-1}.
\end{aligned}
$$

Adaptive FAS Multigrid: The Stiffness Matrix

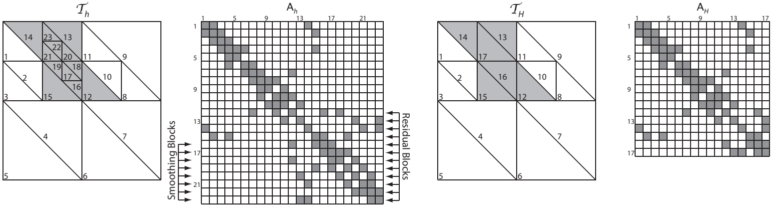

Figure: A two-level hierarchical mesh and corresponding stiffness matrices represented in element-wise block form.

Ω_S: the union of triangles 16 through 23 from $\mathcal{T}_h$. (The new highest level triangles)
Ω_R: the union of triangles 12 through 23 in $\mathcal{T}_h$ (the grey region).

For the sake of efficiency, smoothing is preformed only on Ω_S; residuals are calculated on Ω_R.

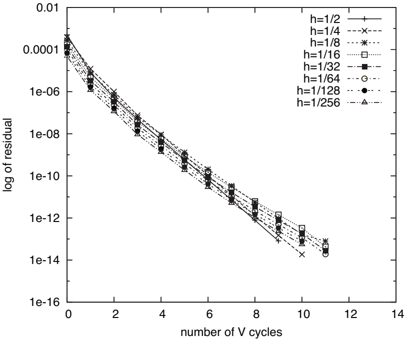

log of residual
number of V cycles
0.01
0.0001
1e-06
1e-08
1e-10
1e-12
1e-14
1e-16
0
2
4
6
8
10
12
14
h=1/2
h=1/4
h=1/8
h=1/16
h=1/32
h=1/64
h=1/128
h=1/256

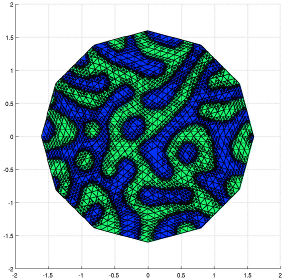

Semi-discrete in time 2nd-order convex splitting scheme for the CH-B equation (formulation in Collins et al., 2013),

$$\psi^{k+1} - \psi^{k} = \tau \nabla \cdot \left(\varepsilon M \left(\tilde{\psi}^{k+\frac{1}{2}} \right) \nabla w^{k+\frac{1}{2}} - \tilde{\psi}^{k+\frac{1}{2}} \mathbf{u}^{k+\frac{1}{2}} \right) \,,$$

$$w^{k+\frac{1}{2}} = \frac{1}{2\varepsilon} \left[\left(\psi^{k+1}\right)^2 + \left(\psi^{k}\right)^2 \right] \psi^{k+\frac{1}{2}} - \frac{1}{\varepsilon} \tilde{\psi}^{k+\frac{1}{2}} - \varepsilon \Delta \hat{\psi}^{k+\frac{1}{2}} \,,$$

$$-\nabla \cdot \left(\nu \left(\tilde{\psi}^{k+\frac{1}{2}} \right) \mathrm{D} \left(\mathbf{u}^{k+\frac{1}{2}} \right) \right) + \eta \left(\tilde{\psi}^{k+\frac{1}{2}} \right) \mathbf{u}^{k+\frac{1}{2}} = -\nabla p^{k+\frac{1}{2}} - \lambda \tilde{\psi}^{k+\frac{1}{2}} \nabla w^{k+\frac{1}{2}} \,,$$

with $\nabla \cdot \mathbf{u}^{k+\frac{1}{2}} = 0$.

Note: For first order convex splitting numerical analysis and implementation see for FD Collins et al., Communications in Computational Physics, 2013 and Guo, Ruihan and Xu, Yan, Journal of Computational Physics, 2015 for LDG method.

Work in Progress for the CH-B

Preliminary Results (not published yet)

This semi-discrete in time and fully discrete SIP-DG-FE CS2 scheme for any time step $\tau > 0$ and for any $\tau > 0$, $h > 0$ respectively is uniquely solvable, energy stable $(E(u^{k+1}) \leq E(u^k))$ and mass conservative, $((u^{k+1}, 1) = (u^k, 1))$ for all $k \geq 0$.

Note

- The above results and theoretical error estimates for a fully discrete SIP-DG formulation is work in progress along with the full adaptive code implementation.
- The methods under study include stabilized DG methods using equal-order spaces for the pressure space and the velocity space.
- A CS2 BDF scheme is in development.

Goal: apply the developed computational tools to more detailed models.

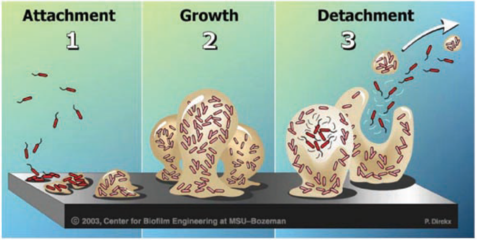

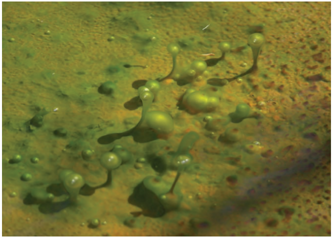

Figure: Left: Stages of the biofilm life cycle, courtesy of the Montana State University Center for Biofilm Engineering, P. Dirckx. Right: Microbial structures in a mixed-species photosynthetic mat, Mushroom Spring, Yellowstone National Park.

[1] Isaac Klapper and Jack Dockery, Mathematical Description of Microbial Biofilms, SIAM Review (2010)

List of Collaborators (for the presented projects)

- Ohannes Karakashian, University of Tennessee Knoxville, Mathematics
- Steven Wise, University of Tennessee, Knoxville, Mathematics
- Isaac Klapper, Temple University, Mathematics

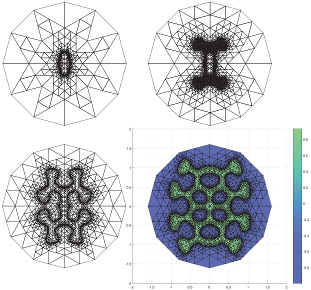

Thanks

NSF-DMS 1720226